Materials and Devices
An International Scientific Journal
OPEN ACCESS
Freely Accessible Scientific Papers.
CA-IP
Managed by scientists for Science - http://co-ac.com

Article type: A-Regular research paper

A DRX Study of the CuAl Layered Double Hydroxide Synthesis Evolution

S. Nieto-Zambrano (1*), E. Ramos-Ramírez (2), F.J. Tzompantzi-Morales (3), N. Gutiérrez-Ortega (4)

(1) Chemistry Department. Laboratory and Catalysis Research and New Materials (LICATUC). Exacts and Natural Science Faculty. University of Cartagena, Cartagena, Colombia, snietoz@unicartagena.edu.co
(2) Preparation, Processing and Characterization of Catalytic and Ceramic Materials / Chemistry Department (DCNE) / University of Guanajuato, Guanajuato, México, ramosre@ugto.mx
(3) Metropolitan Autonomous University – Iztapalapa, Chemistry Department. San Rafael Atlixco. Avenue # 186. México. 09340 D.F., fjtz@xanum.uam.mx
(4) Department of Civil and Environmental Engineering, Engineering Division, Guanajuato Campus, University of Guanajuato. 77th Juarez St. Downtown. Guanajuato, GTO, C.P. 36000. México, normagut@ugto.mx

***Corresponding author: snietoz@unicartagena.edu.co**

RECEIVED: 28 April 2024 / RECEIVED IN FINAL FORM: 27 August 2024 / ACCEPTED: 2 September 2024

Abstract: Copper/Aluminum Layered Double Hydroxide phase (CuAl LDH) has been synthesized with low percentage of impurities to use it as photoredox catalyst, templating agent for nanohybrid-photocatalysts, in CO_2 storage and its abatement and/or highly efficient semiconductor. $Cu(NO_3)_2.2.5H_2O$ and $Al(NO_3)_3.9H_2O$ with Na_2CO_3 and NaOH under variable pH-coprecipitation, reacted. At constant low $CO_3^{2-}/Cu^{2+} + Al^{3+}$, basic pH and ageing time (96h) with slight variations in temperature, resulted in a mix of malachite, CuAl LDH and traces of $Cu(OH)_2$ phases, mainly. At basic pH and fixed temperature with different ageing time, similar XRD patterns were acquired with marked differences, though. When the $CO_3^{2-}/Cu^{2+} + Al^{3+}$, ageing time, and pH were constant (7.50, 96 h, 9.24), small changes in temperature led to variations in the diffractograms and the band gap energy of the obtained finest LDH, fell in the visible spectrum. A more precise tuning of the conditions has led to comprehend better their influence in the LDH formation, which is important in defining the role of the active part in chemical process and the solid real applications.

Keywords: CuAl LDH, SYNTHESIS IMPROVEMENT, XRD PATTERNS, CARBONATE RATIO, BAND GAP ENERGY.

Cite this article: S, Nieto-Zambrano, E. Ramos-Ramirez, F.J. Tzompantzi-Morales, N. Gutierrez-Ortega, OAJ Materials and Devices, Vol 8, 1408-p1 (2024) - DOI: 10.23647/ca.md20241408

Introduction

Synthesis of hydrotalcites (H) or Layered Double Hydroxides (LDH) is registered back as 1942 with Feitknech and his preparation of the first LDH starting with aqueous metal salt solutions and base (**Feitknecht, 1942**). Later, other researchers have been obtaining it, perhaps by 7 different ways. **Miyata & Kumura (1973)**, reported synthetic variables and characteristic anion exchange (gas molecules) and molecular sieving properties of different LDH. Varying M^{2+} and M^{3+} cation or the anion (changing the interlayer distance) of the precursors and considering certain rules involving a limited range in product solubilities differences (Kps of $M^{2+}(OH)_2$ and $M^{2+}(A^{n-})_{2/n}$) and metal ion radius proximity, they achieved the formation of LDH phases. **Miyata (1975)**, mostly focused on MgAl LDH and synthesis through coprecipitation at constant pH (10 ± 0.2) and its exchange properties studies by varying the anion of the precursor (NO_3^-, Cl^-, ClO_4^-, CO_3^{2-}) and using different analytical techniques to characterize and study them (XRD, SEM, elemental analysis, TGA, IR Spectroscopy, surface area by BET method and acidity-basicity determination). **Reichle (1986)**, synthesized different LDH systems by varying the nature of M^{2+} and M^{3+}, M^{2+}/M^{3+} molar ratio, solution pH (8-11) and analyzed the results of crystallization temperature and time modifications in the morphology and particle size. **Sato et al. (1988)**, obtained LDH of different M^{2+} and M^{3+} (Mg^{2+}, Ni^{2+}, Co^{2+}; Al^{3+}, Fe^{3+} and CO_3^{2-} as anion) by coprecipitation and studied some of their physico-chemical properties (solid solubility limit of M^{3+}, thermal decomposition, reconstitution reaction mechanism and solubility in water at 25°C). **Trifiro et al. (1988)**, centered their work in obtaining CuAl LDH and analyzed the role of preparation method and the ions involved in such synthesis. By calcination, LDH gave rise to a well dispersed and stable oxides. Authors of this study, analyzed the effect of the M^{3+} in the H surface area and porosity. **Yamaoka et al. (1989)**, attempted to obtain CuAl LDH using as precipitating agent Na_2CO_3 2M solution and a mixture of the metallic precursor of 0.1 M $Cu(NO_3)_2$ and $Al(NO_3)_3$ at different molar ratio of $Cu^{2+}/Cu^{2+} + Al^{3+}$ and $CO_3^{2-}/Cu^{2+} + Al^{3+}$ and studied their anion exchange properties with mono and divalent anions. In general review, **Cavani et al. (1991)**, wrote an exhaustive analysis of the state of the art of LDH or hydrotalcite (H) type anionic clays in reference to synthesis methods, properties, and applications. **Costantino et al. (1998)**, carried out the preparation of LDH with Al^{3+} and varied the M^{2+} (Mg^{2+}, Ni^{2+}, Zn^{2+}) by thermally induced hydrolysis of urea, analyzed the results in composition and crystallinity and researched their exchange features using Cl^- and alkoxides anions in the presence of the respective alkanols, which led to formation of a bilayer of extended alkyl chain in the interlayer region of the particular MgAl LDH. **Lwin et al. (2001)**, focused on synthesis of CuAl LDH by sequential precipitation using Na_2CO_3 as a mineralizing agent and metal nitrates as precursors. They varied the molar ratio of Cu^{2+}/Al^{3+} between 0.5 – 4.0 and under 0.5, obtained malachite phase. Above and under that molar ratio range, amorphous phase Al species occurred, also. After XRD of the dried precipitate, they obtained LDH phase as the major component in all products. **Trujillano et al. (2006a)**, addressed the preparation and physico-chemical properties of CuAl LDH through coprecipitation at constant pH of 8.3 using a solution of NaOH 1.0 M with a molar ratio of 2.0 with metallic nitrates. Such suspension was stirred for 24 h in air, centrifuged, washed, and dried at room temperature. Additionally, they studied the intercalation of diverse surfactants. The three following reviews, render a summary about preparation methods and important applications, such as **Nalawade et al. (2009),** who wrote analytically on the important applications of LDH in drug delivery since most negatively charged biomolecules can be incorporated between the LDH hydroxide layers by exchange, thus promoting the growing of that area of research in nanohybrids. **Nishimura et al. (2013)**, reviewed advancements in characterization and synthesis to get highly functionalized LDH for heterogeneous catalysts performing in key reactions such as value-added chemical synthesis (biomass derived materials) and **Conterosito et al. (2018),** described a compendious revision of the advancements in LDH preparation methods (hydrothermal, sol-gel, urea, ion exchange, rehydration, coprecipitation, microwave/sonication methods). Furthermore, general properties of these compounds have been examined **(Miyata, 1983)**, **(Reichle, 1985), (Misra, 1992), (Cavani et al., 1991), (Rives et al., 2014)** and their interest is driven by their use as absorbent for CO_2, ion exchange host, drug delivery hosts, precursors for multicomponents catalysts and photocatalyst, polymer/LDH nanocomposites, besides of having a low cost, memory effects and easy for recycling. Moreover, thanks to semiconducting properties, it is possible to regulate the electronic density at the interfaces or in the interaction limit of M^{2+}-M^{3+} **(Yamaoka et al., 1989), (Rives et al., 2001), (Kannan et al., 2004), (Trujillano et al., 2006a), (Mizugaki et al., 2013), (Tokudome et al., 2016), (Li et al., 2017)**, **(Wang et al., 2018)**, **(Yi et al., 2019)**, **(Aragaw et al., 2022), (Z. Li et al., 2023), (Han et al., 2023), (Lokesh & Srivastava, 2023)**. Additionally, thermal treatment of these lamellar compounds produces mixed metal oxides with high stability and dispersion of the metal **(Cavani et al. 1991).** Additionally, their controlled calcination leads to mixed oxides with peculiar acid-base properties plus synergetic effects that enhance chemical activity **(Reichle et al., 1986), (Ginés et al., 1995), (Balduzzi et al., 2001), (Crivello et al., 2005), (Takehira & Shishido, 2007), (Lwin & Abdullah, 2009), (Balsamo et al., 2012), (Chakraborty et al., 2015), (Abderrazek et al., 2016).**

LDH, hydrotalcites (H) or anionic clays consists of layers organized like in the brucite ($Mg(OH)_2$) structure. This is pillared with layers that are formed by the sharing of the edges of octahedra of $M^{2+}(OH)_6$, where M^{2+} is in the center. The formula of the LDH is $[M^{2+}{}_{(1-x)}\ M^{3+}{}_{(x)}\ (OH)_2]^{x+}\ [A_{x/n}]^{n-}.mH_2O$, where M^{2+} and M^{3+} are divalent and trivalent ions, respectively **(Ayala et al., 2011)**. Isomorphic substitution of the M^{2+} by M^{3+} in the mentioned octahedra occurs and generates a positive charge, which is counterbalanced by A (interlayer anion, such as CO_3^{2-}, NO_3^-, halides, etc) and H_2O molecules. The ions should comply with the ratio of $[M^{3+}/\ M^{2+} + M^{3+}]$ among 0.2 – 0.4 **(Cavani et al., 1991), (Evans & Slade, 2006), (Nalawade et al., 2009), (Martín Del Campo et al., 2011), (Forano et al., 2013)**. See Figure 1.

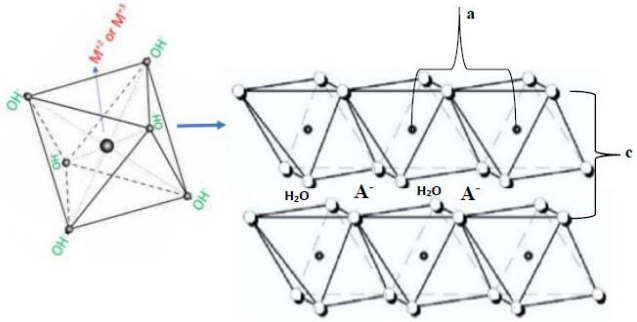

Figure 1. Chemical Layered Structure of an LDH.

There have been various reported methods of CuAl LDH preparation. For instance, **Herman et al. (1978),** published

the preparation of amorphous CuAl LDH from the decomposition of a copper ammoniacal complex on γ-Al_2O_3. **Reichle (1986),** reported the formation of CuAl-CO_3^{2-} LDH when a gel was obtained using a bicarbonate solution as precipitant at high temperature. Besides, coprecipitation at variable and constant pH of metal nitrates mixtures using NaOH-Na_2CO_3 or $NaHCO_3$-Na_2CO_3 as precipitant solution, has been commonly used and provided a pH which favors Cu and Al precipitation **(Miyata, 1980), (Yamaoka et al., 1989), (Alejandre et al., 1999), (Likhar et al., 2009), (Ichikawa & Miyazoe, 2011), (Yan et al., 2013), (D. Li et al., 2018)**. Additionally, various authors have published that divalent ion from Mg^{2+} to Zn^{2+} form LDH like materials, except Cu^{2+}, due to Jahn-Teller effect. Some authors have suggested and introduced a second M^{2+} ion during synthesis to mitigate such effect, though obtaining a ternary LDH **(Busetto et al., 1984), (Alejandre et al., 1999), (Schwenk & Rode, 2003), (Chaboy et al., 2006), (Vorontsova et al., 2007).** Otherwise, it will most probably result in mixed phases, low purity, and yield. Therefore, it is difficult to find the precise conditions for binary CuAl LDH synthesis. Hence, depending on the routes and synthesis conditions, different crystalline phases can be formed, hence, it becomes a challenge to clarify the contribution of each one in chemical processes (**Reichle et al., 1986), (Trifiro et al., 1988), (Yamaoka et al., 1989),** (**Schwenk & Rode, 2003), (Kannan et al., 2004), (Köckerling et al., 1997), (Reinen et al., 1997), (Merlini et al., 2012). Behrens & Schlögl (2013)**, reported that only a tiny change in pH or T had an enormous effect in the resulting metastable material when they tried to obtain Cu/ZnO catalyst for methanol production. Also, they agreed that synthesis conditions during early precipitation and ageing steps turned out to be central for catalytic properties. From their work, it could be inferred a similarity in the mechanism for CuAl LDH and Cu/ZnO catalyst forming. Malachite ($Cu_2(OH)_2(CO_3)$), gerhardtite ($Cu_2(NO_3)(OH)_3$), $Cu(OH)_2$ including metal oxides, were reported by these authors, as well. Notwithstanding, several investigators have reported the synthesis of binary CuAl LDH. For instance, **Alejandre et al. (1999),** brought into an amorphous CuAl LDH and tried its calcined product in the photocatalysis of phenol. They used triethylamine as precipitant agent, while **Yamaoka et al. (1989)** used a 2 M Na_2CO_3 solution in a mixture of $Cu(NO_3)_2$ and $Al(NO_3)_3$ with different molar ratios of Cu^{2+}/Al^{3+} and carbonated ratio (CO^{2-}_3/Cu^{2+} $+Al^{3+}$). **Behrens & Schlögl (2013),** reported precipitation pH ranges of the cations Cu^{+2} and Zn^{+2} and predicted where the co-precipitation of these ions will be greater with dependence on the ratio of the molar fraction ($CO^{=}_3$ **/** (Cu^{2+} + Al^{3+}) and the volume of Na_2CO_3 used as precipitant agent.

The study of this CuAl LDH synthesis has been attended and looked for adjusting the experimental laboratory conditions to get the CuAl LDH to use it alone or as hybrid form for CO_2 storage, photocatalysis and renewable energy and at the same time, clarify its formation and fill the shortages in the description of the steps in the way to its obtention. It is well known that this CuAl LDH synthesis is easily altered by the preparation variables (different to MgAl LDH that is easier replicated, for instance), which can be attributed to a low enthalpy of formation of the respective hydroxides and higher solubility of the LDH. Hence, it is difficult to turn out the simultaneous coprecipitation of the $Cu(OH)_2$ and $Al(OH)_3$ into a CuAl LDH because more than two synchronized parameters, control the obtention mechanism and come into play to determine the final product with the structure, crystallinity and level of purity that could serve for any required purposes with the needed key functionalities. The thermodynamic of this metastable CuAl LDH makes it difficult to fine and tune the precise conditions that allow to get a major percentage of the hydrotalcite phase. That being the case, the role of the preparation conditions of CuAl LDH synthesis was investigated here with the purpose of optimizing them to accomplish Cu-Al-CO_3 LDH as pure as possible with lower carbonate ratio. Varying pH, T, and ageing time, a thoroughgoing CuAl LDH synthetic study was performed, and the most crucial tryout sets are presented in this report. Scarce literature has reported a detailed synthetic task results as the present work, related to this CuAl LDH. The improved product will be used as LDH functional materials alone, calcined or integrated to nanoparticles. In future contribution, we are planning to use them as a multicomponent catalyst and /or templating agent in the design of nanohybrid composites photocatalysts for final use in renewable energy, environmental remediation, and electronic applications. Hence, despite of previous publications on CuAl synthesis, there is still space for improving the LDH stability, which depends on very fine-tune adjusting of preparation variables. The synthesis conditions described in table 1, were selected after a throughout consultation of the state of the art related to CuAl hydrotalcites preparation and some preliminary experimentation.

Table 1. Variables of CuAl LDH Synthesis.

T°C	pH	a.t.	Precursors W(g)	W(g)	N
65.0	9.20	24 h	12.0781g Cu^{+2} 6.2278g Al^{+3}	6.2748g	A1
75.0	9.20	24 h	12.0782g Cu^{+2} 6.2271g Al^{+3}	5.9669g	A2
85.0	9.20	24 h	12.0789g Cu^{+2} 6.2272g Al^{+3}	6.2087g	A3
72.0	8.00	96 h	12.0790g Cu^{+2} 6.2271g Al^{+3}	6.8000g	B1
74.0	9.24	96 h	12.0734g Cu^{+2} 6.2283g Al^{+3}	6.1000g	B2
77.0	11.16	96 h	12.859g Cu^{+2} 6.2279g Al^{+3}	3.9000g	B3
71.0	9.24	96 h	11.6315g Cu^{+2} 6.2283g Al^{+3}	6.3801g	C1
75.0	9.24	96 h	11.6299g Cu^{+2} 6.2288g Al^{+3}	6.4588g	C2
77.0	9.24	96 h	11.6312g Cu^{+2} 6.2281g Al^{+3}	6.6182g	C3
65.0	9.21	48 h	11.6371g Cu^{+2} 6.2275gAl^{+3}	6.7103g	D1
70.6	9.24	48 h	11.6329g Cu^{+2} 6.2276gAl^{+3}	6.6380g	D2
74.0	9.24	48 h	11.6304g Cu^{+2} 6.2271gAl^{+3}	6.7872g	D3

All synthesis had a constant molar ratio of Cu^{+2}/Al^{+3} = 3; N: nomenclature; W(g): weight; a.t.: ageing time; n: moles.

More than one paper has demonstrated the high predominance of the pH in the LDH synthesis. For instance, **Haraketi et al. (2017),** evidenced that at acidic conditions, no hydrotalcite structure is formed, nevertheless, for a Cu^{2+}/Al^{3+} molar ratio of 3, samples prepared within the range 9-11 showed a XRD pattern like those of hydrotalcite and they manifested that such pH depends on the cations used. According to the consulted literature, pure CuAl LDH can most probably be synthesized with a Cu^{2+}/Al^{3+} molar ratio of 3, without discarding a molar ratio range of most probably obtention. Furthermore, at this ratio, various authors have attained diffractograms which exhibit characteristic peak of the LDH structure and if such ratio increased, other phases were registered as oxides, copper hydroxide ($Cu(OH)_2$), aluminum hydroxides ($Al(OH)_3$) **(Haraketi et al., 2017), (Abderrazek et al., 2016)**. For low pH, no hydrotalcites phase were observed, however, CuO and $Al(OH)_3$ were presented. Also, pH greater than 10 promotes formation of additional phases such as sodium tetrahydroxycuprate due to amphoteric properties of copper

oxide and as a result the formation of $[Cu(OH)_4]$. As our reading progressed, it was concluded that under or over pH around 9, part of Cu^{2+} and Al^{3+} remained in solution and precipitation was incomplete **(Yamaoka et al., 1989), (Behrens & Schlögl, 2013).** For these reasons, at first, our experimental synthesis was based on the 2 most dominant parameters (pH and Cu^{2+}/Al^{3+} molar ratio of 3 and from preliminaries and results of experimental set A, conditions were implemented for the rest of the series.

2. Materials and Methods

2.1. Chemicals: the following materials were used as received: $Cu(NO_3)_2.2.5H_2O$ (Sigma Aldrich), $Al(NO_3)_3.9H_2O$ (Fermont), Na_2CO_3 (Reasol), NaOH (Reasol), miliQ deionized H_2O, labware.

2.2. Synthesis Methodology: the LDH was prepared by coprecipitation for the higher scaling up feasibility (or down) and tendency to excellent purity and crystallinity **(Bukhtiyarova, 2019).** The mixture of metallic salts $Cu(NO_3)_2.2.5H_2O$ and $Al(NO_3)_3.9H_2O$ with Cu^{2+}/Al^{3+} constant molar ratio equal to 3, was done at a variable pH. The conditions of pH, T, and ageing time (a.t.) were varied. After adjusting pH with a solution mixture of Na_2CO_3 and NaOH ($\frac{X_{Na2CO3}}{Y_{NaOH}}) = 0.66$ equivalent to a carbonate molar fraction of 7.51 ($\frac{n_{CO3\,2-}}{n_{Cu2++Al3+}}$), the reaction system was kept in reflux with constant stirring. The product was separated from the mother solution and washed exhaustively with 500 mL portions of hot deionized water. The solid was dried at 80 °C, pulverized and stored in a vial. The synthesis conditions are described in table 1.

2.3. Characterizations: X-ray diffractograms were measured using a Brucker D2 Phaser diffractometer with CuKα radiation (λ= 0.15405 nm). It used a generator power of 30 kV and 10 mA under Positive Sensitive Detector (PSD) continuous fast mode. The analysis was carried out over a range of 2θ between 10-70 ◦ with a step size of 0.02 ◦ and 2s counting time. The sample with the most similar XRD pattern was selected for further characterization by UV-Vis spectroscopy, The molar ratio of the solid was quantified with Perkin-Elmer model Optima 3200 Dual Vision by Inductively Coupled Plasma Atomic Emission Spectrometry and Scanning Electron Microscopy coupled to Energy Dispersive Spectroscopy (SEM-EDS). SEM was carried out with a scanning electron microscope from Carl-Zeiss and acceleration voltage of 40 kV. The sample was placed on carbon film and mounted on a conventional holder. Additionally, the UV Vis−NIR absorption spectra were performed on a Varian Cary 100 UV-Vis NIR spectrophotometer with an integration sphere to carry out UV-VIS Spectroscopy coupled with Diffuse Reflectance Spectroscopy (DRS). The instrument was set to a 2 nm bandwidth and 200-800 nm range. The data was processed using Cary Eclipse software. The band gap of the material was determined by plotting the Kubelka-Munk function versus its UV-Vis absorption energy. Thermogravimetric TGA and Differential thermal (DTA) analysis were performed on a TA Instrument SDT Q600. 5 mg sample was heated at a ramp of 10 °/min up to 1100 °C with a 20 mL/min air flow and α-alumina as standard reference. The specific surface area of the sample was acquired with a TriStart II Plus 2.03 from Micromeritics by N_2 adsorption isotherms.

3. Results and Discussion

For group A, T was varied from 65 to 85 ° C. For these 3 syntheses (constant pH of 9.20, ageing time (a.t.) of 24 h), the XRD patterns were analogous (see Figure 2). If main peaks are observed in these diffractograms (set A), malachite $Cu_2(OH)_2CO_3$ (JCPDS No. 41-1390) as the main phase, $Cu(OH)_2$ (JCPDS No. 13-420), and LDH phase (compared to the LDH standard JCPDS No. 089-5434) of very weak intensity can be identified **(Muñoz et al., 2015; Ramos-Ramírez et al., 2018).** In addition, the higher the temperature the greater the intensity of the malachite phase XRD reflections (A3). LDH phase XRD reflections could not be predominant, though. Furthe more, the intensity of the XRD signals for $Cu(OH)_2$ were low. In the A set, T did not substantially alter the diffraction pattern when the a.t. and pH were kept constant, as evidenced by the similarity of the diffractograms A1, A2 and A3. This can be explained as there was not enough time to crystallize well and evolve to LDH structure, though, there was a change in T.

In group B, the a.t. were constant (96h) while pH and T were varied. Under conditions B1, the best XRD pattern match was the malachite phase (JCPDS No. 41-1390, red rectangles in Figure 2). The product obtained with conditions B2 (74°C / pH9.24 / 96h) was analogous to JCPDS No. 037-0630, corresponding to the LDH $Cu_6Al_2(OH)_{16}CO_3.4H_2O$ phase, with few weak impurities of $Cu(OH)_2$, confirming a CuAl LDH product with significant amount of hydrotalcite phase (green triangles in fig.2). This one is presented here as the CuAl LDH with the best LDH XRD features. The LDH characteristic reflection at 11.90 (2θ), was clearly observed in B2, however, changes in T and pH marked significant differences in diffractograms B1 and B3. For B3 conditions, the best similarity was $Cu(OH)_2$. The evolution of the XRD patterns for the samples of series B shows that when increasing both T and pH while the aging time remains constant, malachite, then malachite and LDH and finally $Cu(OH)_2$ phases were completely formed. On the other hand, comparing samples A2, B2 and D3, it is shown that at the same T and pH, when raising the aging time, the phases move from malachite and few LDH (A2, 24h), LDH and few malachite (D3, 48h) and finally to LDH and few $Cu(OH)_2$ (B2, 96h). These results suggested that malachite, CuAl LDH and $Cu(OH)_2$ are successfully formed when either T and pH or aging time are increased. According to **Behrens & Schlögl (2013),** higher pH (greater than 9.0) leads to irreversible oxolation (CuO). They performed a titration curve (pH versus Volume of Na_2CO_3 or $n_{CO3}{}^{2-}/n_{Cu}{}^{2+}{}_{or\ Zn}{}^{2+}$; n are moles) for Cu^{2+}, Zn^{2+} and Al^{3+} and inferred that to assure complete precipitation of Cu^{2+} and Al^{3+} (cations of interest in this work), the pH should not be lower than 5.0 neither higher than pH 9.0 because in high caustic solution, oxolation occurs and transforms the product to $Cu(OH)_2$ and finally to a stable CuO. Additionally, at acidic pH, broad peaks are obtained due to reflections at similar 2θ values as for brucite, leading to low crystalline hydroxides instead of hydrotalcite **(Kloprogge et al., 2004).**

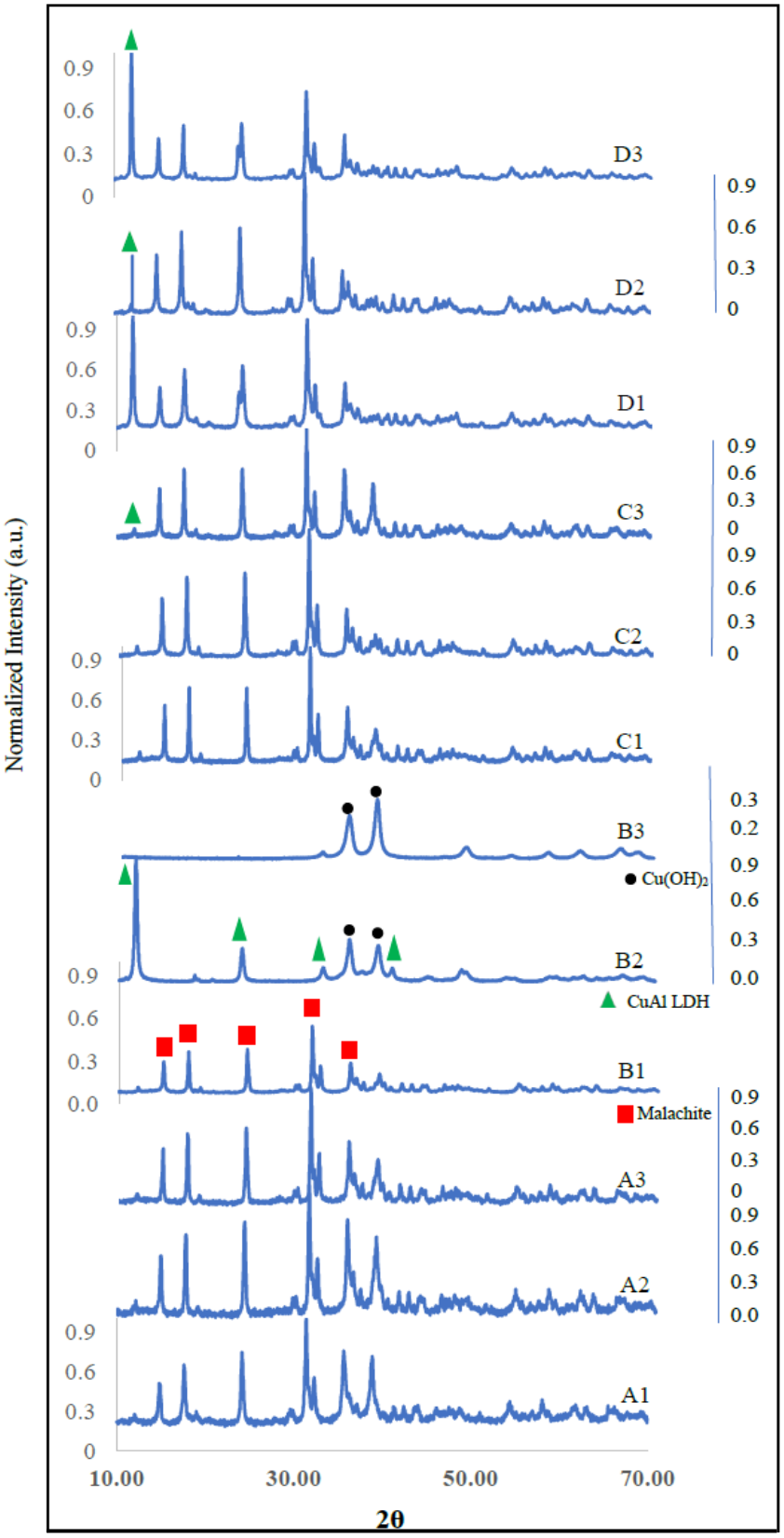

Figure 2. Diffractograms of the Obtained Product.

Group C was carried out at a constant pH and ageing time 0f 9.24 and 96 h(respectively) with variable T of 71, 75 and 77ºC. In these cases, a large part of the XRD signals corresponded to malachite and were comparable to the resulting of set A. These signals did not have a notable change when T increased (C1 to C3), under these conditions, corroborating the outcomes of set A. At a fixed molar ratio, the proper selection of pH and T are decisive to complete precipitation. Having mentioned this, an optimum pH can be certain within a T range. This gets support on the work of **Behrens & Schlögl (2013)**, because on their titration curve, they located a precipitation plateau for each cation (Cu^{2+}, Zn^{2+} and Al^{3+}) as a function of temperature. They observed that a decrease in T moves such plateau to higher pH and vice versa. Hence, the Cu and Al content of the precursors mixed solutions will not precipitate if the pH is further low at a given T or the contrary. This goes along with the observation that once the pH has been adjusted, T can be key in the obtention of the LDH structure. The diffractograms evolutions for series A and C, exhibited that increasing only T did not modify the nature of the crystalline phases.

Group D was carried out at constant a.t. and pH with 48h and 9.24, respectively. Although the presence of malachite was noted at 70.6 ° C (D2), the signal for LDH at this T is undoubted [main reflection at 11.90 (2θ)] and it showed higher intensity at 74 ° C (D3). The reflection at 11.90 (2θ) for LDH stood out under these conditions, although it does not exceed neither intensity nor purity to the one obtained under B2 conditions. For D set, the LDH signal intensity diminished in D2 and increased in D3, which can be explained by the difference in T that favored crystallization. In this set, the changing variable was T while pH and a.t. were kept in 9.24 and 48 h, respectively. Additional correlation of set A, C and D, put forward that the optimum ageing time for LDH formation is 48 hours.

Not obtaining the LDH phase with the A set (T was the only variable), can mainly be attributed to ageing time, which is associated to crystallization, and this affects the size and morphology of the particles. Moving to B set (there were 2 variables pH and T), the ageing time was constant but increased to 96 compared to A set where the a.t. was 24 h. For this B set, changes in pH were the cause of distinctive crystalline structure since modifications in T of 2 – 3 °C can affect, however, not predominantly the outcomes of the synthesis. The effect of pH is clear when samples of B series are compared. Although T increases slightly, it is distinguishable that high or low pH supports the formation of malachite and $Cu(OH)_2$ and taking this into account, the LDH structure is most probably formed at intermediates pH. With B2 conditions, a clearer LDH XRD features were generated and allowed us to establish the most assertive pH of 9.24 with a T of 74°C. The C set leaves us in disappointment because a slight difference in T with the same a.t. as B set, did not allow to get the LDH XRD characteristics. This can be due to the small difference in T that provoked variations on the precipitation plateau, therefore, it could also have been needed a modification in the pH, most probably. Lastly, for D set, the pH was kept at 9.24 and changes in T like in B2 with diminution in a.t. to 48 h, produced a solid with prevailing LDH XRD features. In this case, two constant conditions were kept and nonetheless, it did not improve its LDH XRD characteristics.

Moreover, if diffractograms B2 and D3 are compared, the difference between them was a modification in the a.t. from 96 h to 48 h and keeping constant pH and T. In this case, LDH structure showed important peaks, however, there was a distinctive mixture with other phases (more notable in D3). Therefore, keeping 2 constant conditions leads to the presence of other phases without disappearing the hydrotalcite structure. Furthermore, any tryout at pH greater than 9.25 will not favor the LDH structure formation. Finally, sample B2 (Figure 3) was chosen for complete characterization.

The crystalline diameter calculated by means of the Debye-Scherrer equation(**Holzwarth & Gibson, 2011**) was 20.13 nm. The cell parameters were calculated using the reflections from planes [003] and [110] with the formula **c**= $3d_{003}$ as related to interlayered distance and **a**= $2d_{110}$ as the metal-metal average distance between the octahedrons of the crystalline lattice. The calculated crystalline red parameters were **c**= 2.282 nm and **a**= 0.301 nm **(Trujillano et al., 2006b), (Velu & Swamy, 1996), (Bravo-Suárez et al., 2004), (Prince et al., 2015)**. The above diffractogram displayed very sharp and symmetric characteristic reflections of the crystallographic planes [003], [006] and [009] with high crystallinity and low impurities (Figure 3).

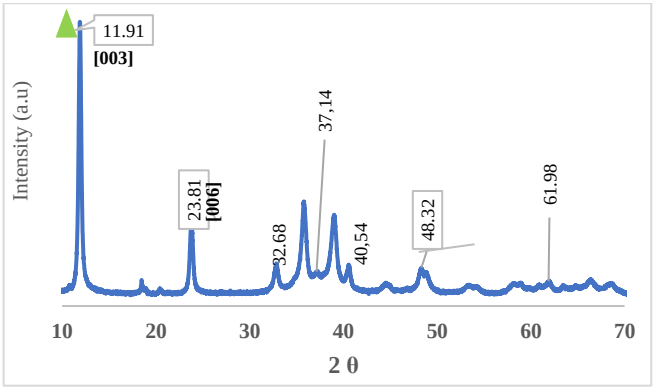

Figure 3. Diffractogram (B2) for CuAl LDH.

Several processes were evidenced during the thermal analysis of the product with the higher percentage of CuAl LDH phase. The first major transition in the thermogravimetric analysis (TGA, Figure 4a) was found between 100.00 – 155.31 °C, which can be connected to the corresponding peak (153°C) in thermodifferential analysis (TDA, blue curve, fig. 4b) with a loss of 8.98 % associated to removal of physisorbed H_2O on the surface of the solid. Between 155.31 and 228.40° C, there was a loss of 5.76 % attributed to removal of interlayered H_2O. A drop of 7.44 % between 228.41 and 580.00°C was related to an endo-peak at approximately 252.19 °C of the TDA due to continued dihydroxylation of the interlayer and initial thermal decomposition of carbonate anions. The next loss between 580.00 – 900.00 °C was 3.40% ascribed to continued decarbonation from the LDH-like phase **(Kannan et al., 2004)**

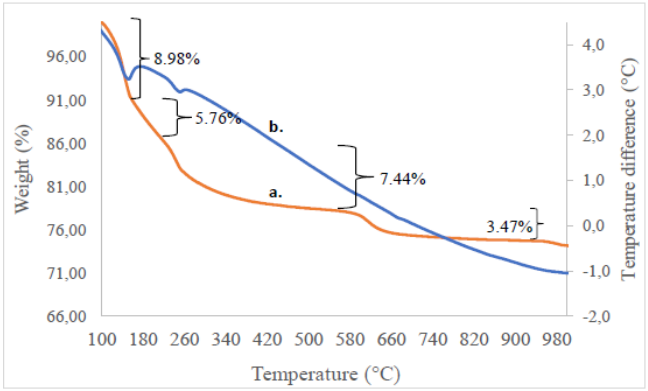

Figure 4. TGA/TDA (a/b respectively) of CuAl LDH. Fresh CuAl LDH b) Calcined CuAl LDH.

(Voyer et al., 2009). The CO_3^{2-} is linked in a mono- and bidentated way to the LDH layers. It has been reported that CO_3^{2} decomposes at low T whilst the bidentated CO_3^{2-} at higher T**(Alejandre et al.,1999).** At around 300.00 °C with the loss of interlayered monodentated CO_3^{2-}, the pillared CuAl LDH started structural collapse and transformation into oxides mixture. The calcined CuAl LDH at 300 °C for 4 hours corresponded to CuO o tenorite according to JCPDS No. 041-254, mainly (see Figure 5).

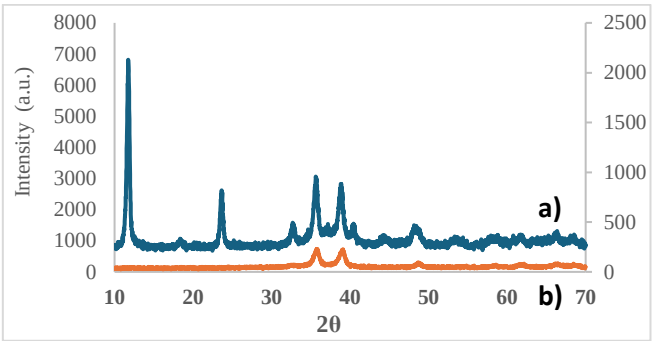

Figure 5. Diffractograms of a) CuAl LDH (B2) and b) calcined CuAl LDH.

Table 2 shows the values of the specific surface area determined by BET method with the physisorption isotherms of N_2 as well as the average pore diameter and volume calculated by Barrett, Joyner and Halenda (BJH) method. The product presented mesopores with average pore diameter of 5.83 nm(Thommes et al., 2015). The liberation of CO_2 and H_2O through thermal decomposition and dehydration in the calcination of the sample (c-CuAl LDH) favored the increase in surface area from 7.41 to 22.40 g/m^2. Moreover, the last column exhibits the divalent to trivalent cation molar ratio determined by ICP-AES. It is inferred a lacking inclusion of the metal cations to the crystalline red of the CuAl LDH, thus the Cu^{2+}/ Al^{3+} was closer to 3.00, though not precisely. The reason for this, could be primarily owed to the different precipitation pH ranges of the two metal cations (Cu^{2+} and Al^{3+}) as can be corroborated in the phase diagram for those metals **(Schweitzer & Pesterfield, 2010), (Prince et al., 2015)**.

Table 2. Textural Analysis Parameter of CuAl-H

Name	A_{BET}	V_{poro} (BJH) cm^3/g	D_{poro} (BJH) (nm)	$\frac{Al^{+3}}{Cu^{+2}+Al^{+3}}$	M^{+2}/M^{+3}
c-CuAl LDH	22.40	0.04	6.32	-	-
CuAl LDH	7.42	0.04	5.83	0.29	~ 2.50

The micrographs (Figure 6) resemble cotton flakes, caused by sheets arranged randomly, exhibited dispersed and appreciable porosity. Small aggregates of 3500-3800 nm are observed. Micrograph of CuAl LDH calcined at 300 ° C (Figure 6b) indicates more defined agglomerates than in the fresh, which is attributed to the dehydroxylation and decarboxylation that at this T has already advanced with remarkable loss of the hydrotalcite-type structure.

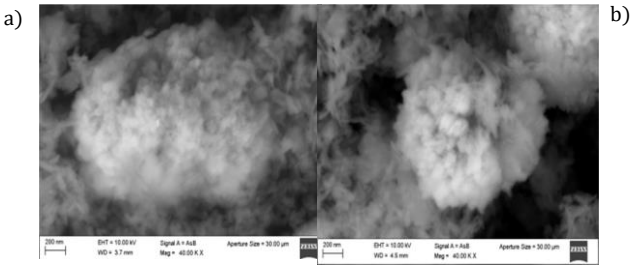

Figure 6. Scanning Electron Microscopy of a) Fresh CuAl LDH b) Calcined CuAl LDH.

The evaluation of the band gap energy (band gap energy, E_g) was carried out using the Kubelka-Munk (KM) function, F (R) = (1-R)^2 / 2R, where R is the reflectance % of the DRS-UV-Vis spectrum **(Landi et al., 2022).** E_g values are reported in table 3, where E_g corresponds to energy mostly in the visible region and compared to the very common TiO_2 and ZnO, the resulting Eg will be more favorable in photocatalysis (see table 3).

Table 3. Band Gap Energies of Obtained Products.

E_g (eV)	Nomenclature
2.91	B1
2.10	B2
1.22	B3
1.34	cB2

c: Calcination at 300 °C

Conclusion

As a conclusion, the handling of variables in the CuAl LDH synthesis are decisive in the outcomes in the CuAl LDH forming. The synthesis pH was set at 9.24 as the more crucial factor in the synthesis, with T of approximately 74°C and a.t. between 48-96h. The final product with the more significant % of the LDH structure, had a band gap energy that fall lower than for the most common solids in photocatalysis, such as ZnO and TiO_2, which could cast successful application in visible photocatalysis. This whole empirical tuning of conditions conducted to a higher degree of optimization of the CuAl LDH phase that could be used alone or integrated to nanoparticles. Particularly, it is expected by the presence of Al^{+3} in the laminar structure of the obtained CuAl LDH, that a sudden recombination will be reduced in photooxidation with visible light and will behave as a tramp for electrons and therefore, a greater time for recombination of the exciton in the synthesized material. This sounds as a good photoactive candidate in assisted processes, such as photooxidation, photoreduction or highly efficient semiconductors materials. Furthermore, this type of investigation conduces to a better understanding and tuning of the precise conditions needed for this metastable hydrotalcite of CuAl.

Acknowledgements:

Sincere thanks to CONACYT (México), University of Guanajuato and Ecocatal Group from Chemistry Department, Metropolitan Autonomous University – Iztapalapa, CDMX (México).

REFERENCES

1. K. Abderrazek, F.S. Najoua, E. Srasra, *Appl Clay Sci*, **vol.119**, p 229 (2016).
2. A. Alejandre, F. Medina, X. Rodriguez, P. Salagre, J. E. Sueiras, *J catal*, **vol. 324**, p. 311 (1999).
3. A. Alejandre, F. Medina, P. Salagre, X. Correig, J. E. Sueiras, *Chem Mat*, **vol. 11**, p. 939 (1999).
4. S. G. Aragaw, G. B. Feysia, N. S. Gultom, D.-H. Kuo, H. Abdullah, X. Chen, O. A. Zelekew, *Appl Water Sci*, **vol. 12**, p140 (2022).
5. A. Ayala, E. Fetterx, G., E. Palomares, P. Bosch, *Mater Lett*, **vol. 65**, p1663 (2011).
6. L. Balduzzi, F.G. Prinetto, Ghiotti, A. Bianchini, M. Livi, A. Vaccari, *In Stud Surf Sci Catal, Oxides-based at the Crossroads of Chemistry*, Elsevier BV, Amsterdam Neherlands, (2001).
7. N. Balsamo, S. Mendieta, M. Oliva, G. Eimer, M. Crivello, *Procedia Materials Science*, **vol. 1**, p506, (2012).
8. M. Behrens, R. Schlögl, *Z Anorg Allg Chem*, **vol. 639**, p2683 (2013).
9. J. J. Bravo-Suárez, E. A. Páez-Mozo, S. T. Oyama, *Quim Nova*, **vol. 27**, p601 (2004).
10. M. V. Bukhtiyarova, *J Solid State Chem*, **vol. 269**, p494 (2019).
11. C. Busetto, v. Del Piero, G. Manara, F. Trifiro, A. Vaccari, *J Catal*, **vol. 266**, p260 (1984).
12. F. Cavani, F. Trifirò, A. Vaccari, *Catal Today*, **vol. 11**, p173 (1991).
13. J. Chaboy, A. Muñoz-Páez, P. J. Merkling, E. S. Marcos, J Phys Chem, **vol. 124**, p1, 2006).
14. Chakraborty, S., Sarkar, I., Haldar, K., S. K.Pal, S. Chakraborty, *Appl Clay Sc, **vol. 107**, p98 (2015).*
15. E. Conterosito, V. Gianotti, Palin, E. Boccaleri, D. Viterbo, M. Milanesio, *Inorgánica Chim Acta,* **vol. 470**, p36 (2018).
16. U. Costantino, F. Marmottini, M. Nocchetti, R. Vivani, *Eur J Inorg Chem*, **vol. 10**, p1439, (1998).
17. M. Crivello, C. Pérez, E. Herrero, G. Ghione, , S. Casuscelli, E. Rodríguez-Castellón, *Catal Today*, **vol.107**, p215 (2005).
18. D. G. Evans,, R. C. T. Slade, *Structure & Bonding*, **vol. 119**, p1, (2006).
19. W. Feitknecht, M. Gerber, *Helv.Chim. Acta,* **vol. 25***, p131, (1942).*
20. C. Forano, U. Costantino, V. Prévot, , C. T. Gueho, In *Dev Clay Sci,* **vol. 5**, p745, (2013).
21. M. J. L. Ginés, N. Amadeo, M. Laborde, , C. R. Apesteguía, *Appl Catal A Gen*, **vol. 131**, p283 (1995).
22. W. Han, H. Hao, Q. Zhang, Z. Shao, *J Environ Chem Eng*, **vol. 11**, p109293, (2023).
23. M. Haraketi, K. Hosni, E. Srasra, *Surf Eng & Appl Electrochem*, **vol. 53**, p360, (2017).
24. Herman, R. G., Klier, K., Simmons, G. W., B. P. Finn, J. B. Bulko, T. P. Kobylinski, *J Catal*, **vol. 56**, p407, (1979),
25. N. Holzwarth, N. Gibson, *Nat Nanotech*, **vol. 6**, p534, (2011).
26. S. Ichikawa, S. Miyazoe, O. Matsuoka, *Chem Lett*, **vol. 40**, p512, (2011).
27. S. Kannan, V. Rives, H. Knözinger, *J Solid State Chem*, **vol.177**, p319, (2004).
28. J. T. Kloprogge, L. Hickey, R. L. Frost, *J Solid State Chem*, **vol. 177**, p4047, (2004).
29. M. Köckerling, G. Geismar, G. Henkel, H.-F. Nolting, *J Chem Soc Faraday Trans, **vol. 93**, p481, (1997).*
30. S. Landi, I. R. Segundo, E. Freitas, M. Vasilevskiy, J. Carneiro, C. J. Tavares, *Solid State Commun*, **vol.341**, p114573, (2022).
31. D. Li, L. Fan, Y. Shen, M. Qi, M. R. Ali, D. Liu, S. Li, *J Nanosci & Nanotech*, **vol. 19**, p1090, (2018).
32. J. Li, S. Zhang, Y. Chen, T. Liu, C. Liu, X. Zhang, M. Yi, Z. Chu, X. Han, *RSC Adv*, **vol. 7**, p29051, (2017).
33. Z. Li, J. Liu, J. Zhao, R. Shi, G. I. N. Waterhouse, X.-D. Wen, T. Zhang, *Adv Func Mat*, **vol. 33**, p2213672, (2023).
34. P. R. Likhar, R. Arundhathi, M. L. Kantam, P. S. Prathima, *Eur J Org Chem*, **vol.31**, p5383, (2009).
35. S. Lokesh, R. Srivastava, *Int J Hydrogen Energy*, **vol. 48**, p35, (2023).
36. Y. win, F. Abdullah, *J Therm Anal Calorim*, **vol. 97**, p885, (2009).
37. Y. Lwin, M. A. Yarmo, Z. Yaakob, A. B. Mohamad, W. R. W. Daud, *Mat Res Bull*, **vol. 36**, p193, (2001).
38. E. Martín Del Campo, J. S. Valente, T. Pavón, R. Romero, Á. Mantilla, R. Natividad, *Ind & Eng Chem Res, **vol. 50**, p11544, (2011).*
39. M. Merlini, N. Perchiazzi, M. Hanfland, A. Bossak, *Acta Crystallogr **B***, **vol. 68**, p266, (2012).
40. C. Misra, *Clays Clay Miner,* **vol. 40***,* p145, (1992).
41. S, Miyata, *Clays Clay Miner,* **vol. 23**, p369, (1975).
42. S. Miyata, *Clays Clay Miner,* **vol. 28**, p50, (1980).
43. S. Miyata, *Clays Clay Miner,* **vol. 31**, p305, (1983).
44. S. Miyata, *Chem Lett,* **vol. 2**, p843, (1973).
45. T. Mizugaki, R. Arundhathi, T. Mitsudome, K. Jitsukawa, K. Kaneda, *Chem Lett*, **vol. 42**, p729, (2013).
46. V. Muñoz, F. M. Z. Zotin, L. A. Palacio, *Catal Today*, **vol. 250**, p173, (2015).
47. P. Nalawade, B. Aware, V.J. Kadam, R. S. Hirlekar, *J Scient Ind Res*, **vol. 68**, p267, (2009).
48. N S. Ishimura, A. Takagaki, K. Ebitani, *Green Chem*, **vol. 15**, p2026, (2013).

49. J. Prince, F. Tzompantzi, G. Mendoza-Damián, F. Hernández-Beltrán, J. S. Valente, *Appl Catal B: Env*, **vol. 163**, p352, (2015).
50. E. Ramos-Ramírez, N. Gutiérrez-Ortega, F. Tzompantzi, C. M. Gómez, G. Del Angel, G. Herrera-Pérez, A. H. Serafín-Muñoz, C. Tzompantzi-Flores, *Adv Mat Sci & Eng*, **vol. 2018**, p8267631, (2018).
51. W. T. Reichle, *J Catal*, **vol. 94**, p547, (1985).
52. W. T. Reichle, *Solid State Ionics,* **vol. 22**, p135, (1986).
53. W. T. Reichle, S. Y. Kang, D.S. Everhardt, J Catal, **vol. 101**, p352, (1986).
54. P. Reinen, H. O. Wellern, J. Wegwerth, *Zeitschrift Fur Physik B-Condensed Matter,* **vol. 104**, p595, (1997).
55. V. Rives, M. del Arco, C. Martín, *Appl Clay Sci*, **vol. 88**, p239, (2014).
56. V. Rives, A. Dubey, S.Kannan, *Phys Chem Chem Phys*, **vol. 3**, p4826, (2001).
57. T. Sato, H. Fujita, T. Endo, M. Shimada, A. Tsunashima, *Reactivity of Solids,* **vol. 5**, p219, (1988).
58. G. K. Schweitzer, L. L. Pesterfield, The Aqueous Chemistry of the Elements, 434 Oxford University Press, NY (2010).
59. C. F. Schwenk, B. M. Rode, *Chem Commun*, **vol. 3**, p1286, (2003).
60. K. Takehira, T. Shishido, *Catalysis Surveys from Asia,* **vol. 11**, p1, (2007).
61. M. Thommes, K. Kaneko, A. V. Neimark, J. P. Olivier, F. Rodriguez-Reinoso, J. Rouquerol, K. S. W. Sing, *Pure and Appl Chem*, **vol. 87**, p1051, (2015).
62. Y. Tokudome, T. Morimoto, N. Tarutani, P. D. Vaz, C. D. Nunes, V. Prevot, G. B. G. Stenning, M. Takahashi, *ACS Nano*, **vol. 10**, p5550, (2016).
63. F. Trifiro, A. Vaccari, G. Del Piero, *Studies in Surface Science and Catalysis,* **vol.39**, p571, (1988).
64. R. Trujillano, M. J. Holgado, F. Pigazo, V. Rives, *Physica B: Condens Matter,* **vol. 373**, p267, (2006A).
65. S. Velu, C. S. Swamy, *Appl Catal A: Gen*, **vol. 145**, p141, (1996).
66. O. A. Vorontsova, R. N. Saenko, O. E. Lebedeva, *Russ J Inor Chem*, **vol. 52**, p1662, (2007).
67. N. Voyer, A. Soisnard, S. J. Palmer, W. N. Martens, R. L. Frost, *J therm Anal & Calorim*, **vol. 96**, p481, (2009).
68. F. Wang, Y. Zhang, W. Liang, L. Chen, Y. Li, X. He, *Sens Actuators B Chem*, **vol. 273**, p41, (2018).
69. T. Yamaoka, M. Abe, M. Tsuji, *Mat Res Bull*, **vol. 24**, p1183, (1989).
70. K. Yan, J. Liao, X. Wu, X. Xie, *Adv Mat Lett*, **vol. 4**, p702, (2013).
71. Yi, Y., Wei, Y., Tsang, P. E., & Fang, Z. *Env Sci & Poll Res*, **vol. 26**, p28361, (2019).